Supporting Information for:

Porosity induced rigidochromism in platinum(II) terpyridyl luminophores immobilized at silica composites

Amie E. Norton,[1,2,*] Kassio P. S. Zanoni,[3,4] Marie-Anne Dourges,[5] Leandro P. Ravaro,[3] Mahmood K. Abdolmaleki,[1,6] Andrea S. S. de Camargo,[3] Thierry Toupance,[5], William B. Connick,[1,a] and Sayandev Chatterjee[7,*]

[1]Department of Chemistry, University of Cincinnati, Cincinnati, OH 45220.
[2]Present Address: USDA-ARS Grain Quality and Structure, 1515 College Ave. Manhattan, KS 66503; *Email: amie.norton@usda.gov.*
[3]Laboratório de Espectroscopia de Materiais Funcionais (LEMAF), Instituto de Física de São Carlos, Universidade de São Paulo, 13566-590, São Carlos – SP, Brazil.
[4]Present Address: Molecular Opto-Electronic Devices (MOED), Instituto de Ciencia Molecular, Parque Cientifico, Universidad de Valencia, 46980 Paterna, Spain.
[5]Univ. Bordeaux, Institute of Molecular Sciences, UMR 5255 CNRS, 351 Cours de la Libération, F-33405 Talence Cédex, France.
[6]Present Address: Department of Biology and Chemistry, Texas A&M International University, Laredo, TX, 78041, USA.
[7]ESSENCE Diagnostics LLC, Livingston, NJ 07039; *Email: sayandev@essencediagnostics.com*
[a]*In memoriam of Dr. William B. Connick who passed away May 18, 2018.*

Content	Pages

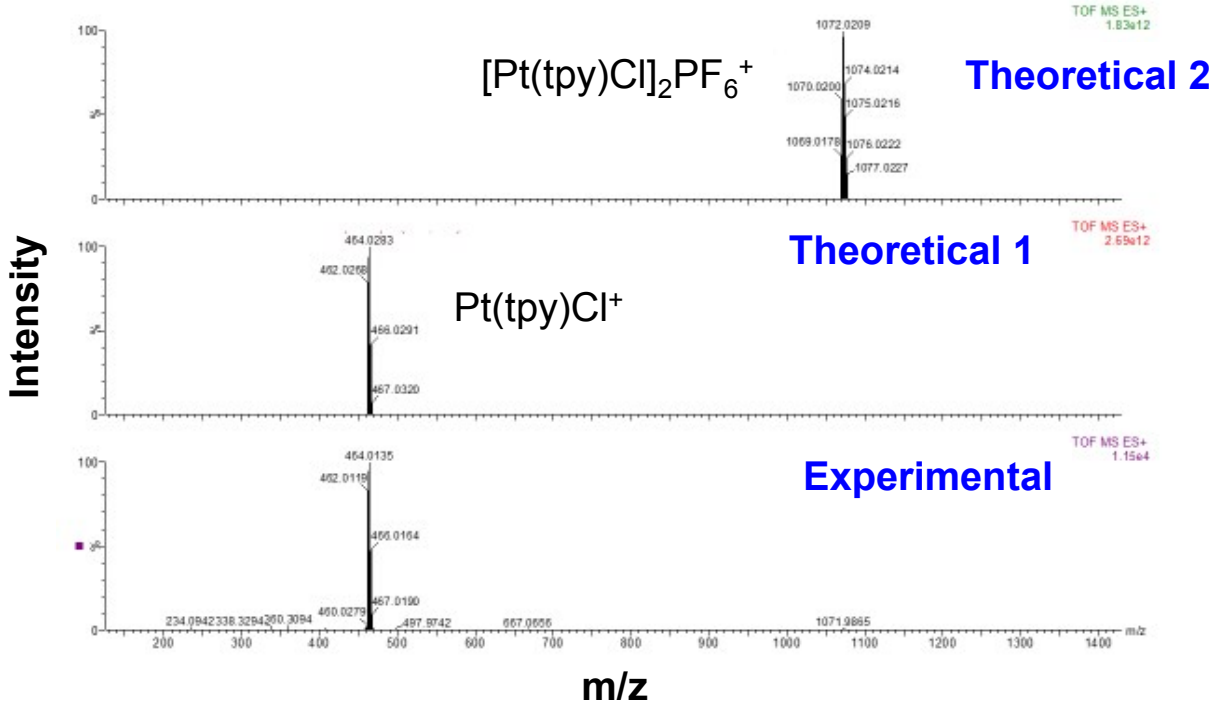

Figure S1. Mass spectrum of **1**•PF_6 post its deposition as a thin film from evaporation of a solution of DMSO:acetone on a microscopic glass slide

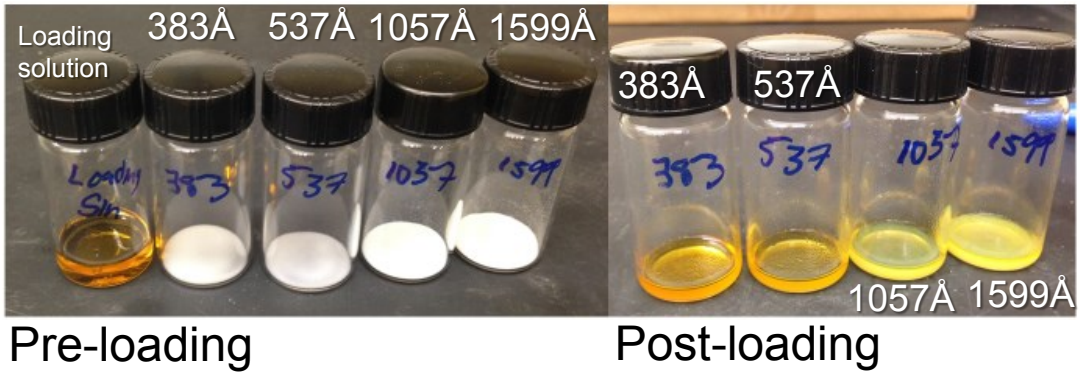

Figure S2. Photographs of (left panel) vials conataining **1**•PF_6 in DMSO:acetone (10 mg/10 ml) and the CPGs pre **1**•PF_6 loading, and (right panel) **1**•PF_6@CPGs post loading. The colors of the **1**•PF_6@CPGs are observed shift to lower wavelengths as the CPG pore size increases.

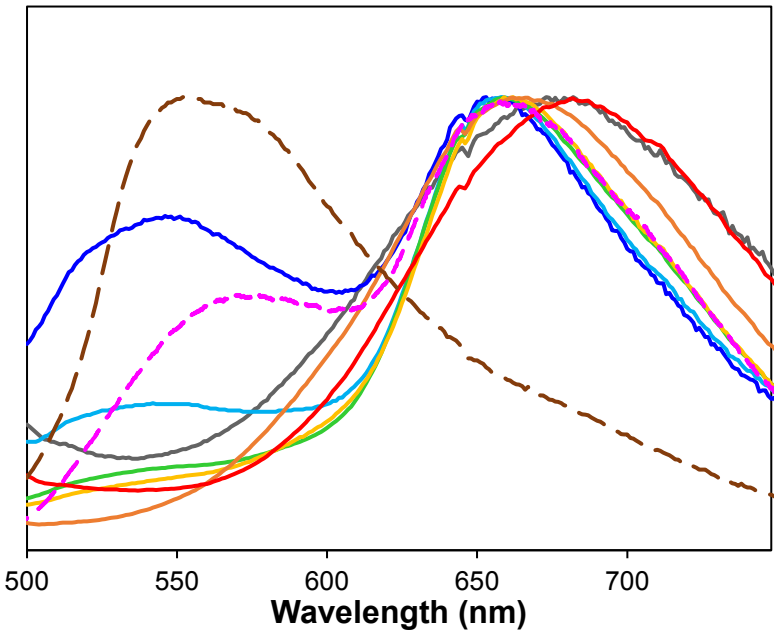

Figure S3. Emsision spectra of **1**•PF_6@silica composites comapred to pristine **1**•PF_6 (λ_{ex}=436 nm). Solid lines: (——) CPG-1599 Å, (——) CPG-1057 Å, (——) CPG-537 Å, (——) CPG-383 Å, (——) CPG-70 Å, (——) MCM-41, (——) NP-SiO_2; dashed lines (– – –)**1**•PF_6 crystalline sample, (– – –) Average large area emission collected using fluorimeter on a thin film of **1**•PF_6 generated from DMSO:acetone solution. The detailed emission on the **1**•PF_6 thin film collected using a laser source is shown in the main paper **Figure 7**.

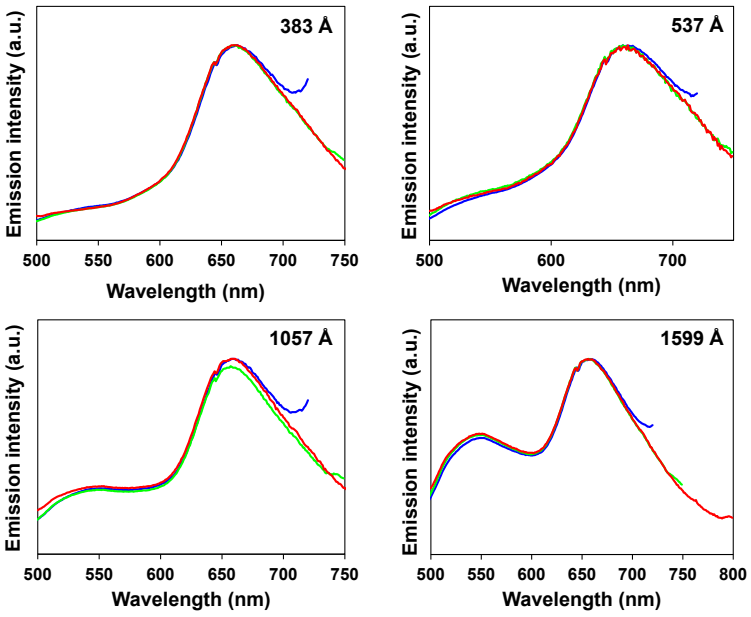

Figure S4. Emission spectra of **1**•PF_6@CPGs excited at different wavelengths (blue) λ_{ex} = 370 nm, (green) λ_{ex} = 410 nm, (red) λ_{ex} = 436 nm.

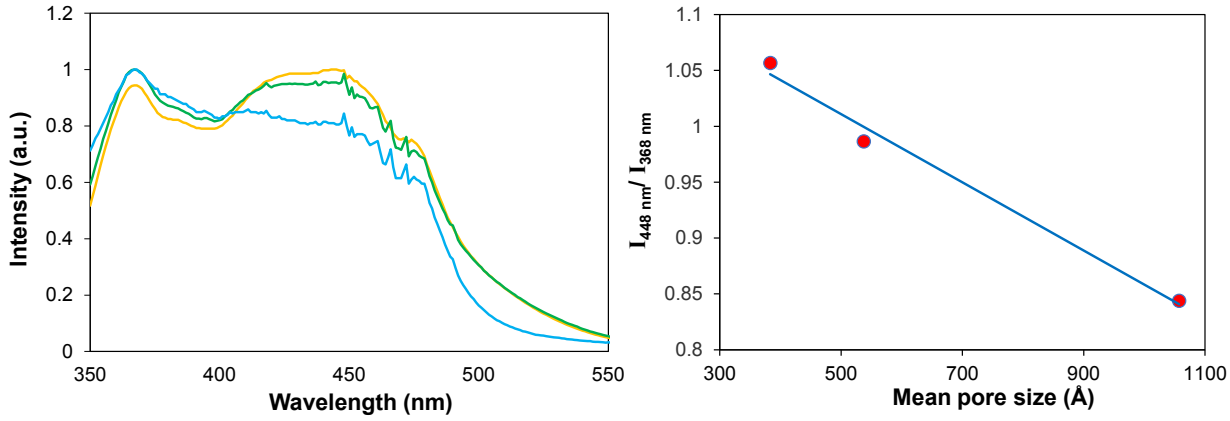

Figure S5. (left panel) Normalized excitation spectra of **1**•PF_6@CPGs monitored at λ_{em} = 550 nm: (——) CPG-1057 Å, (——) CPG-537 Å, (——) CPG-383 Å. (right panel) Ratio of the excitation bands at 448/368 vs pore size. The equation of the line: $I_{448\ nm}/I_{368\ nm}$ = -0.0003×pore size + 1.1637.

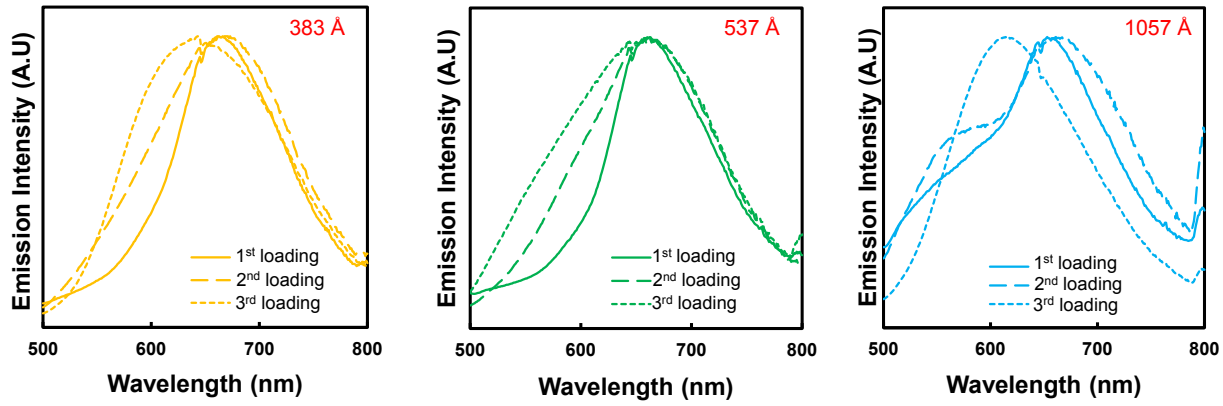

Figure S6. Emission spectra of **1**•PF_6@CPGs over 3 cycles of **1**•PF_6 loading onto the CPGs recorded after each cycle (λ_{ex} = 436 nm)

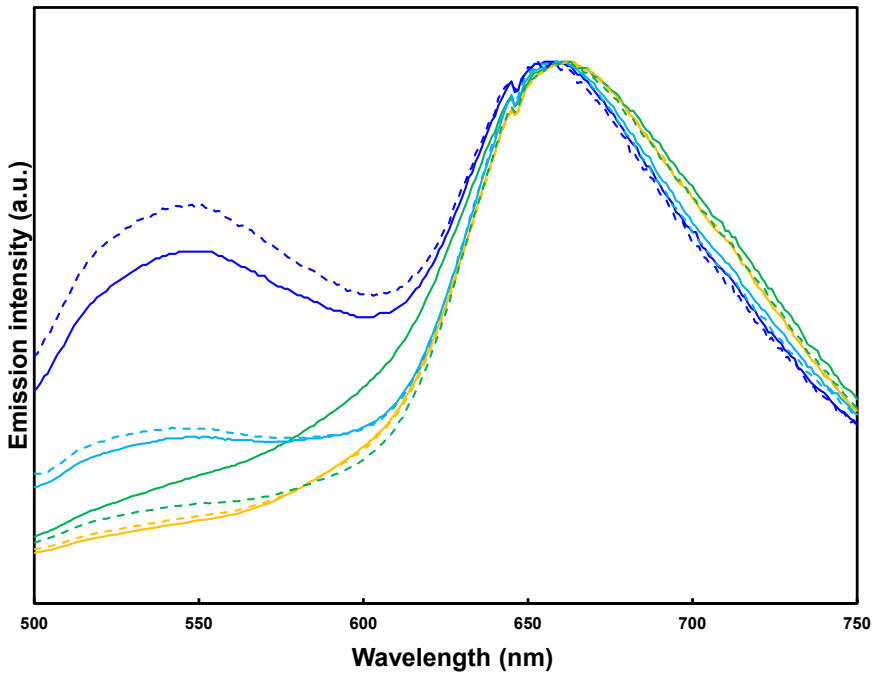

Figure S7. Emission spectra of **1**•PF_6@CPGs (λ_{ex} = 436 nm) based on drying times post **1**•PF_6 loading: (——) CPG-1599 Å, (——) CPG-1057 Å, (——) CPG-537 Å, (——) CPG-383 Å. (solid lines) dried for 4 hours and (dashed lines) dried for 12 hours.

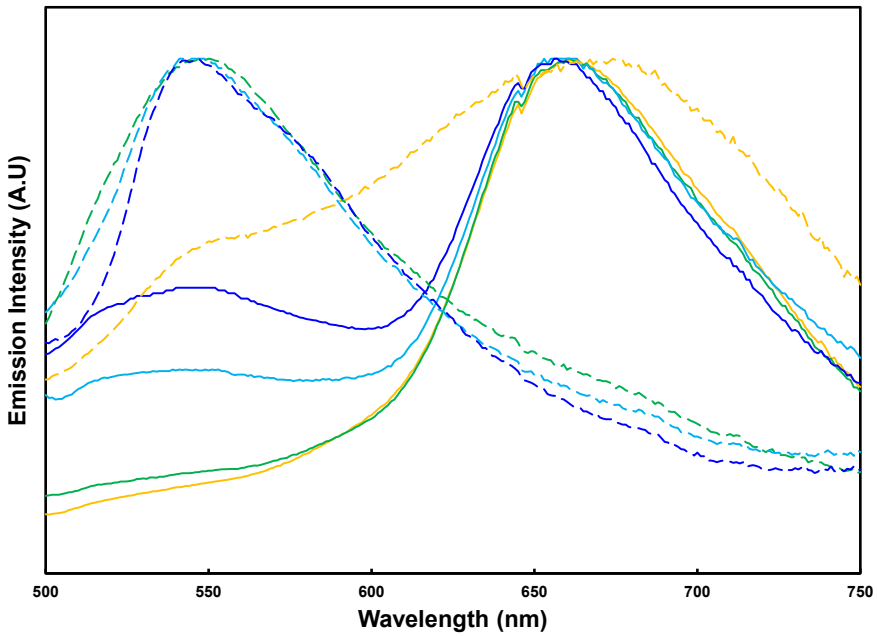

Figure S8. Emission spectra of **1**•PF_6@CPGs (λ_{ex} = 436 nm) with different solvents used for **1**•PF_6 loading: (——) CPG-1599 Å, (——) CPG-1057 Å, (——) CPG-537 Å, (——) CPG-383 Å. (solid lines) **1**•PF_6 loading from DMSO:acetone and (dashed lines) **1**•PF_6 loading from water:acetone

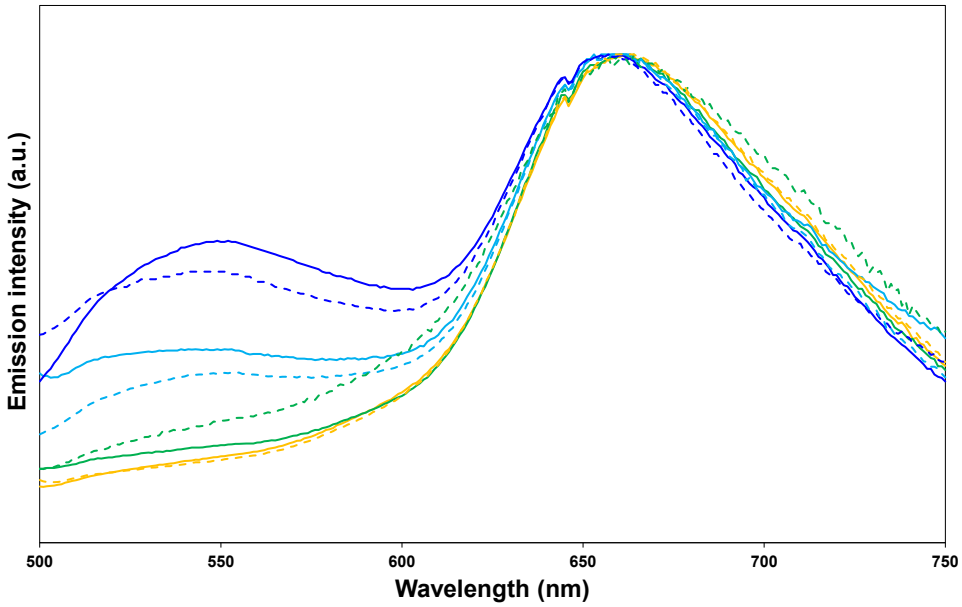

Figure S9. Emission spectra of **1**•PF_6@CPGs (λ_{ex} = 436 nm) recorded at different times: (——) CPG-1599 Å, (——) CPG-1057 Å, (——) CPG-537 Å, (——) CPG-383 Å. (solid lines) spectra collected within 15 minutes post **1**•PF_6 loading from DMSO:acetone and (dashed lines) spectra collected after 7 days post **1**•PF_6 loading from DMSO:acetone

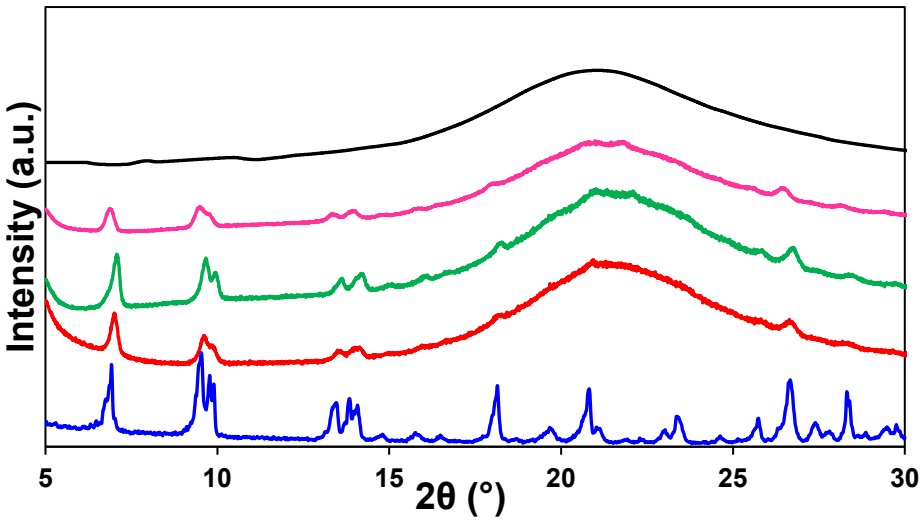

Figure S10. X-ray powder diffractograms of **1**•PF_6@CPGs: (top black trace) blank CPGs, (second from top purple trace) **1**•PF_6@CPG-1599, (third from top green trace) **1**•PF_6@CPG-1057, (second from bottom red trace) **1**•PF_6@CPG-383, (bottom blue trace) pristine **1**•PF_6.

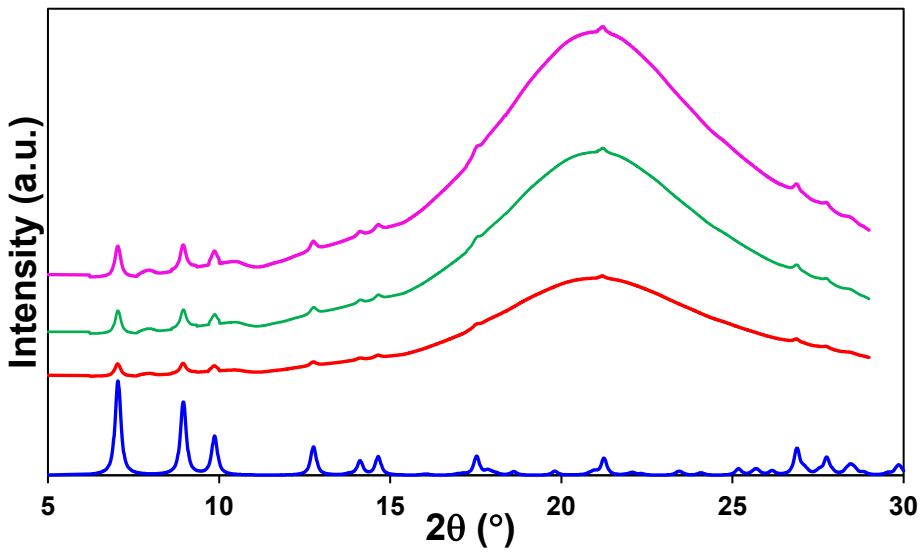

Figure S11. X-ray powder diffractograms of **1**•ClO_4•H_2O: (top purple trace) **1**•ClO_4•H_2O@CPG -1599, (second from top green trace) **1**•ClO_4•H_2O@CPG -1057, (second from bottom red trace) **1**•ClO_4•H_2O@CPG-383, (bottom blue trace) pristine **1**•ClO_4•H_2O.

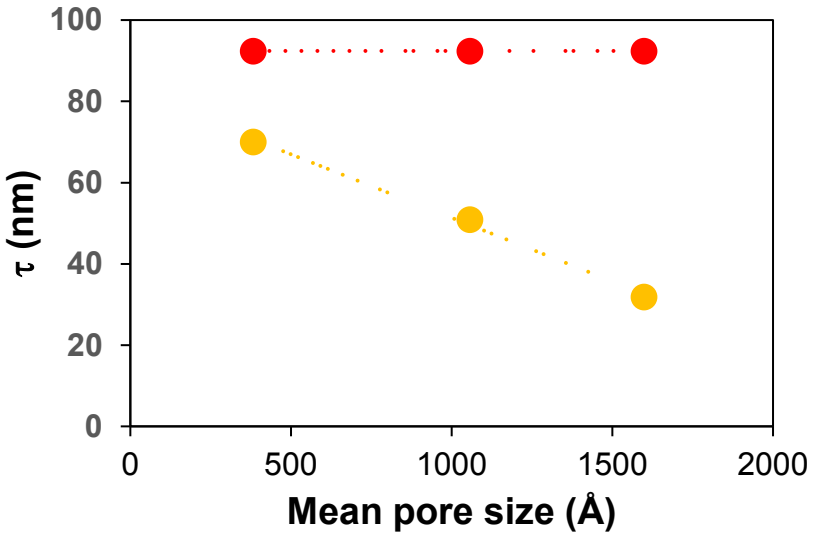

Figure S12. A plot of the mean size of the ordered crystalline domains calculated using Scherrer equation versus the mean pore sizes of the CPGs. (red symbols and trace) **1**•ClO_4•H_2O@CPGs (the analysis done at 6.2°); equation of the line: τ (nm) = -10^{-16} ×(mean pore size, Å) + 92.4; (yellow symbols and trace) **1**•PF_6@CPGs; equation of the line: τ (nm) = -0.03 ×(mean pore size, Å) + 82.6 (the analysis done at 6°)

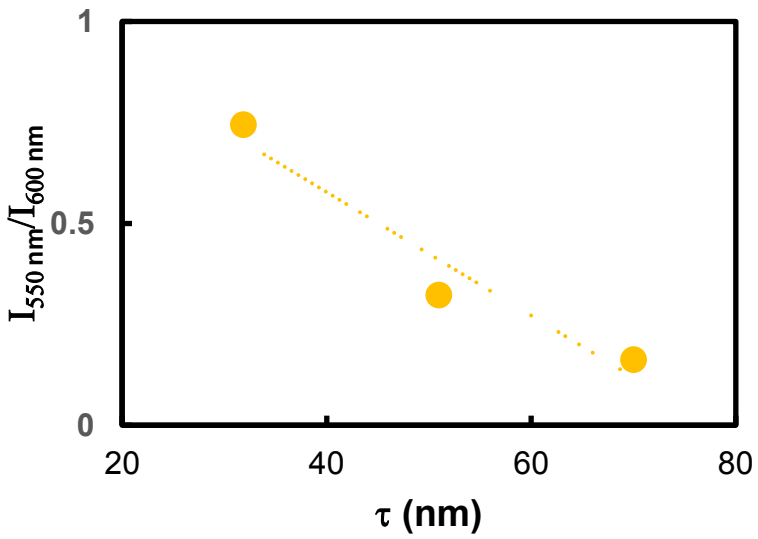

Figure S13. A plot of the ratios of the intensity ratios of the ~550 nm and the ~650 nm emission bands for **1**•PF_6@CPGs (λ_{ex}=436 nm) versus the mean size of the ordered crystalline domains calculated using Scherrer equation; equation of the line: $I_{550\ nm}/I_{630\ nm} = -0.015 \times \tau\ (nm) + 1.19$.